E-ISSN 2656-8039

INTERNATIONAL JOURNAL OF
ENVIRONMENT, ENGINEERING & EDUCATION

VOL. 5, NO. 1, 2023


www.ijeedu.com

Research Article

# Analysis of Land Surface Temperature Distribution in Response to Land Use Land Cover Change in Agroforestry Dominated Area, Gedeo Zone, Southern Ethiopia

**Wendwesen Taddesse Sahile[1], Gashaw Kibret Goshem[1], Seid Ali Shifaw[1], Muh. Rais Abidin[2]**

[1]Department of Land Administration and Surveying, College of Agriculture and Natural Resource Management, Dilla University, Ethiopia

[2]Department of Geography, Universitas Negeri Makassar, South Sulawesi, Indonesia

***Received:*** *February 1, 2023;* ***Accepted:*** *April 15, 2023;* ***Published:*** *April 27, 2023*

**Abstract:** This study examined LST distribution in Ethiopia's agroforestry-dominated Gedeo Zone due to Land Use Land Cover change. For 2005, 2011, 2017, and 2022, 10 m Sentinel 2A and 30 m Landsat images were used to extract and map LST and LULC distribution. The DOS1 method corrected atmospheric errors in all satellite images. LULC change was detected using SVM image classification. The study result revealed that the Agroforestry and Built-up coverage has increased by 1520 sq. km and 2600 sq. km, respectively, from 2005 to 2022. The Bare Land and Farm Land coverage decreased by 1554 sq. km and 2565 sq. km, respectively, in the same period. The LST result has shown that there has been a remarkable variation in the spatial pattern of the LST between 2005 and 2022. The average LST in Agroforestry, Bare Land, Farm Land, and Built-up area has progressively increased over the years, from 19.6°C, 26.0°C, 20.2°C, and 25.58°C in 2005 to 25°C, 32.16°C, 28.23°C, and 30.62 °C in 2022, respectively. While in 2005, the maximum recorded LST did not exceed 37.3°C, by 2022, it had increased by close to 3°C, reaching 40.6°C. The overall result revealed that the average LST in °C has increased from 2005 to 2022. From the result, it was concluded that agroforestry had contributed a lot to LST distribution. LST may not depend on the local LULC change only; other factors like urbanization and global warming could play a significant role in changing LST locally and globally.

**Keywords:** Agroforestry; Dark Object Substruction; Gedeo Zone; Sentinel-2A; Support Vector Machine.

## 1. Introduction

Land surface temperature (LST) measures the earth's surface temperature and is an essential variable in climate modeling and environmental monitoring [1], [2]. It is affected by various factors, including solar radiation, air temperature, humidity, wind speed, and surface properties such as albedo and emissivity [3]. Land Use Land Cover (LULC) changes can significantly impact LST by altering the surface properties and energy balance [4], [5]. Studies showed that converting forested areas to agricultural land results in decreased evapotranspiration and increased surface temperature due to reduced vegetation cover and increased soil exposure [6]–[8].

Agroforestry systems are becoming increasingly popular in many world regions as a sustainable approach to land use management [9]. Introducing agroforestry practices can increase vegetation cover and soil moisture retention and reduce surface temperature [8], [10]. Agroforestry systems can potentially mitigate the adverse effects of LULC changes and provide multiple benefits, including climate adaptation and mitigation, food security, and biodiversity conservation [11]. Agroforestry practice in the Gedeo zone of southern Ethiopia is known as old-aged and indigenous [10]. Gedeo agroforestry is a well-known

**This article citation:** W. T. Sahile, G. K. Goshem, S. A. Shifaw, M. R. Abidin, "Analysis of Land Surface Temperature Distribution in Response to Land Use Land Cover Change in Agroforestry Dominated Area, Gedeo Zone, Southern Ethiopia," Int. J. Environ. Eng. Educ., Vol. 5, No. 1, pp. 19-26, 2023.
**Corresponding author:** Wendwesen Taddesse Sahile (wendwesent@du.edu.et); **DOI:** https://doi.org/10.55151/ijeedu.v5i1.98

land-use system, and it is believed to have self-sustaining and self-regulating attributes compared to other land-use systems in the area [11].

Agroforestry is a climate-smart farming system that is stronger in mitigating climate change than seasonal cropping [12] and gets people nearby to safe working areas for food security from the climate change perspective [13]. LST measures the earth's surface temperature and is an essential variable in climate modeling and environmental monitoring [14]. It is affected by various factors, including solar radiation, air temperature, humidity, wind speed, and surface properties such as albedo and emissivity [15]. Most artificial activities are the leading cause of the constantly declining vegetation cover of the earth's surface [16] and contribute to the rise of LST.

Even though several studies were conducted to observe the impact of LULC change on LST, the extent and direction of these changes remain poorly understood, and there is a need to investigate the impact of LULC on LST in the agroforestry-dominated Gedeo Zone. Understanding the impact of LULC on LST can help identify areas where agricultural productivity may be at risk and guide the development of appropriate adaptation strategies.

In comparing agroforestry systems and subsistence farming, agroforestry systems outperform subsistence farming [12]. The sale of numerous products acquired through the system could result in financial gain [13]. Fruits, nuts, timber, medicinal plants, animal feed, green manure, resins, gum, spices, and other supplementary or diversified items can only be harvested from an agroforestry system, which is especially useful for smallholder farmers [14].

It is an ancient and indigenous agroforestry practice in the Gedeo zone of southern Ethiopia [15]. A well-known land-use system is the Gedeo agroforests, which are thought to be more self-sustaining and self-regulating than other regional land-use patterns [16]. The factors that affect the diversity and composition of agroforestry in the Gedeo zone and elsewhere in Ethiopia have been studied, as have the management of indigenous agroforestry methods, the interaction of agroforestry system components, and other related issues [17], [18].

The extent and direction of these changes remain poorly understood, and there is a need to investigate the impact of LULC on LST in the agroforestry-dominated Gedeo Zone. Understanding the impact of LULC on LST can help identify areas where agricultural productivity may be at risk and guide the development of appropriate adaptation strategies.

## 2. Material and Methods

### 2.1. An Explanation of the Research Site

All the research was done in Ethiopia's Gedeo zone, part of the Southern Nations Nationalities and Peoples (SNNP) region. The geographical range covered by the investigation extends from 5°53′ N to 6°27′ N and from 38° 8′E to 38°30′E in latitude and longitude, respectively (Figure 1). This area is between 1,500 and 3,000 meters above sea level. Annual precipitation averages between 800 and 1800 mm, and average annual temperatures range from 12.5 to 25 degrees Celsius in this region [19].

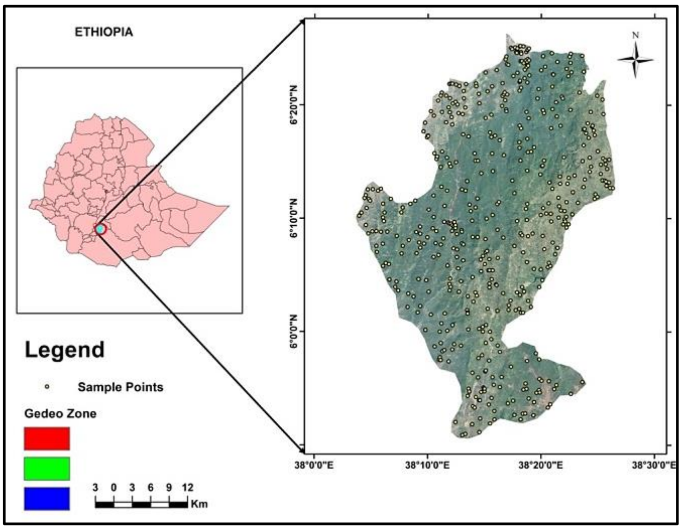


**Figure 1.** Location of the Study Area Showing the Distribution of Points Used in Accuracy Assessment.

### 2.2. Data Sources

Two years of Cloud-free Sentinel-2A MSI images were downloaded from European Space Agency (ESA) website for land use land cover classification in 2017 and 2022. Sentinel image has a 10 m spatial resolution relatively higher resolution than Landsat images. Three scenes of sentinel images were mosaicked and subset to the study area to address the extent of the study area. Additionally, four years of Landsat imageries with a path/row 168/56 were downloaded from the USGS-EROS website (https://eros.usgs.gov/) for land cover classification and LST extraction. A 1.50 m and 5.00 m spatial resolution Spot images and Google Earth historical images were utilized for assessing the accuracy of classification for 2005, 2011, and 2017.

**Table 1.** Data Sources of Research

| Sensors Names | Acquisition Date | Spatial Resolution (m) | Cloud cover (%) | Sources |
|---|---|---|---|---|
| TM | 01/01/2005 | 30.00 | 0.00 | USGS |

| Sensors Names | Acquisition Date | Spatial Resolution (m) | Cloud cover (%) | Sources |
|---|---|---|---|---|
| ETM+ | 01/01/2011 | 30.00 | 0.00 | USGS |
| OLI_TIRS | 01/01/2017 | 30.00 | 0.00 | USGS |
| OLI_TIRS | 01/01/2022 | 30.00 | 0.00 | USGS |
| Sentinel 2A | 01/01/2017 | 10.00 | 0.02 | ESA |
| Sentinel 2A | 01/01/2022 | 10.00 | 0.02 | ESA |
| Spot 5 | 2005 | 5.00 | - | GII |
| Spot 7 | 2017 | 1.50 | - | GII |

### 2.3. LULC Mapping and Accuracy Assessment

The Dark Object Subtraction (DOS1) method, located in Quantum GIS 3.10's preprocessing tool, removed atmospheric distortion from the previous satellite images before the classification began. The land cover maps for 2017 and 2022 were derived from 10 m reflective bands of Sentinel 2A and 30 m Landsat 5, 7, and 8 images for 2005 and 2011 using a Support Vector Machine (SVM) classification algorithm. The SVM is a commonly used supervised machine learning algorithm widely used for classification techniques for image classification [20]. Accordingly, four classification classes (Agroforestry, Bare land, Built-up, and Farmland) were identified in the study area. The SVM was preferred due to its higher performance than other classifiers [21]. One hundred representative GPS points were collected from each LULC class to assess the classification accuracy in January 2022.

### 2.4. Land Surface Temperature Retrieval

LST extraction from Landsat images involves converting the digital numbers (DN) values in the thermal band of Landsat imagery into LST values [22]. Landsat sensors' thermal band measures the radiation emitted from the earth's surface in the thermal infrared wavelength range [23], [24].

#### *2.4.1. Conversion of DN to Radiance*

The raw DN values in the thermal band of Landsat images are not directly proportional to the emitted radiance from the earth's surface [25]. The DN values were first converted to radiance using radiometric calibration coefficients provided by the USGS [23].

$$\mathbf{l\lambda} = (\boldsymbol{LMAX\lambda} - \boldsymbol{LMIN\lambda})/(\boldsymbol{QCALMAX} - \boldsymbol{QCALMIN}) * (\boldsymbol{QCAL} - \boldsymbol{QCALMIN}) + \mathbf{LMIN\lambda} \quad (1)$$

where: Lλ = Spectral Radiance; QCAL = the quantized calibrated pixel value in DN; LMINλ = the spectral radiance that is scaled to QCALMIN); LMAXλ = the spectral radiance that is scaled to QCALMAX); QCALMIN = The minimum quantized calibrated pixel value (1); QCALMAX = the maximum quantized calibrated pixel value (255).

Utilizing the rescaling factors stored in the metadata file, the following equation was used to convert DN values to Radiance for OLI-TIRS.

$$\boldsymbol{L\lambda} = \boldsymbol{MP} \times \boldsymbol{QCAL} + \boldsymbol{AL} \quad (2)$$

where: Lλ = TOA planetary Spectral Reflectance; AL = Reflectance additive scaling factor for the band; QCAL = L1 pixel value in DN; MP = Reflectance multiplicative scaling factor for the band.

#### *2.4.2. Conversion of Radiance to Sensor TB*

TB was calculated by equation 1 from the spectral radiance of thermal bands [24], [26].

$$\mathbf{TB} = \frac{\boldsymbol{K2}}{\boldsymbol{Ln}\left(\frac{\boldsymbol{K1}}{\boldsymbol{L\lambda}} + \mathbf{1}\right)} \quad (3)$$

where: TB = brightness temperature (K); Lλ = TOA spectral radiance; K1 = calibration constant 1; and K2 = Calibration Constant 2, (Table 2).

**Table 2.** TM, ETM+, and TIRS Thermal Bands Calibration Constants.

| Sensor | Band | K1 | K2 |
|---|---|---|---|
| Landsat 7 ETM+ | Band 6 | 666.09 | 1278.71 |
| Landsat 8 TIRS | Band 10 | 777.8853 | 1321.0789 |
| Landsat 8 TIRS | Band 11 | 480.8883 | 1201.1442 |

Determining the Emissivity of the Land Surface: Emissivity is closely related to the Normalized Difference Vegetation Index (NDVI), and can be calculated using the following formula. [24], [27].

$$\varepsilon = \mathbf{0.004} \times \boldsymbol{Pv} + \mathbf{0.986} \quad (4)$$

where: ε = Land surface emissivity; P*v* - Proportion of vegetation, and was calculated by the formula [28].

Finally, LST was computed from the emissivity using equation 2 [29]:

$$\mathbf{LST} = \left(\frac{\boldsymbol{TB}}{(\mathbf{1} + (\boldsymbol{\lambda} \times \boldsymbol{\rho})\ \mathbf{n}\ \boldsymbol{\varepsilon})}\right) \quad (5)$$

where: LST = Land Surface Temperature; TB = Brightness Temperature in Kelvin; λ = Wavelength of the emitted radiance (11.457 for TM and 11.269 for ETM+); $\varepsilon$ = land surface emissivity; ρ = 〖1.438^(-2) mK.

For the split-window algorithm, ε was calculated by equation [24]:

$$\varepsilon = \varepsilon s \times (1 - FVC) + \varepsilon v \times FVC \quad (6)$$

where: ε = Land surface emissivity; εs = Emissivity for soil; εv = Emissivity for vegetation (Table 3); FVC = Fractional Vegetation Cover and calculated from NDVI [24].

**Table 3.** Emissivity Values of Soil and Vegetation

| Emissivity | Band 10 | Band 11 |
|---|---|---|
| εs | 0.971 | 0.977 |
| εv | 0.987 | 0.989 |

Using a split-window algorithm, LST was calculated by:

$$LST = TB_{10} + C1(TB_{10} - TB_{11}) + C2(TB_{10} - TB_{11})^2 + C0 + (C3 + C4W)(1 - m\varepsilon) + C5 + C6W)\Delta\varepsilon \quad (7)$$

where: $TB_{10}$ and $TB_{11}$ = Brightness Temperature of Band 10 and 11; $C_0$, $C_1$, $C_2$, $C_3$, $C_4$, $C_5$, and $C_6$ = Split Window coefficient values are shown in (Table 4); m$\varepsilon$ = LSE Mean; Δ$\varepsilon$ = LSE difference; and W = Atmospheric water vapor content.

**Table 4.** Split Window Algorithm Constant Values

| Constants | C0 | C1 | C2 | C3 | C4 | C5 | C6 |
|---|---|---|---|---|---|---|---|
| Values | 0.268 | 1.378 | 0.183 | 54.300 | -2.238 | -129.200 | 16.400 |

Independently, LSE for band 10 and band 11 was computed. Then, the mean and the difference of LSE were computed by equations [30].

$$m\varepsilon = \frac{LSEb10 + LSEb11}{2} \quad (8)$$

$$\Delta\,\varepsilon = LSEb10 - LSEb1 \quad (9)$$

Conversion LST from the kelvin to degree Celsius

$$LST(celsius) = LST(Kelvin) - 273.15 \quad (10)$$

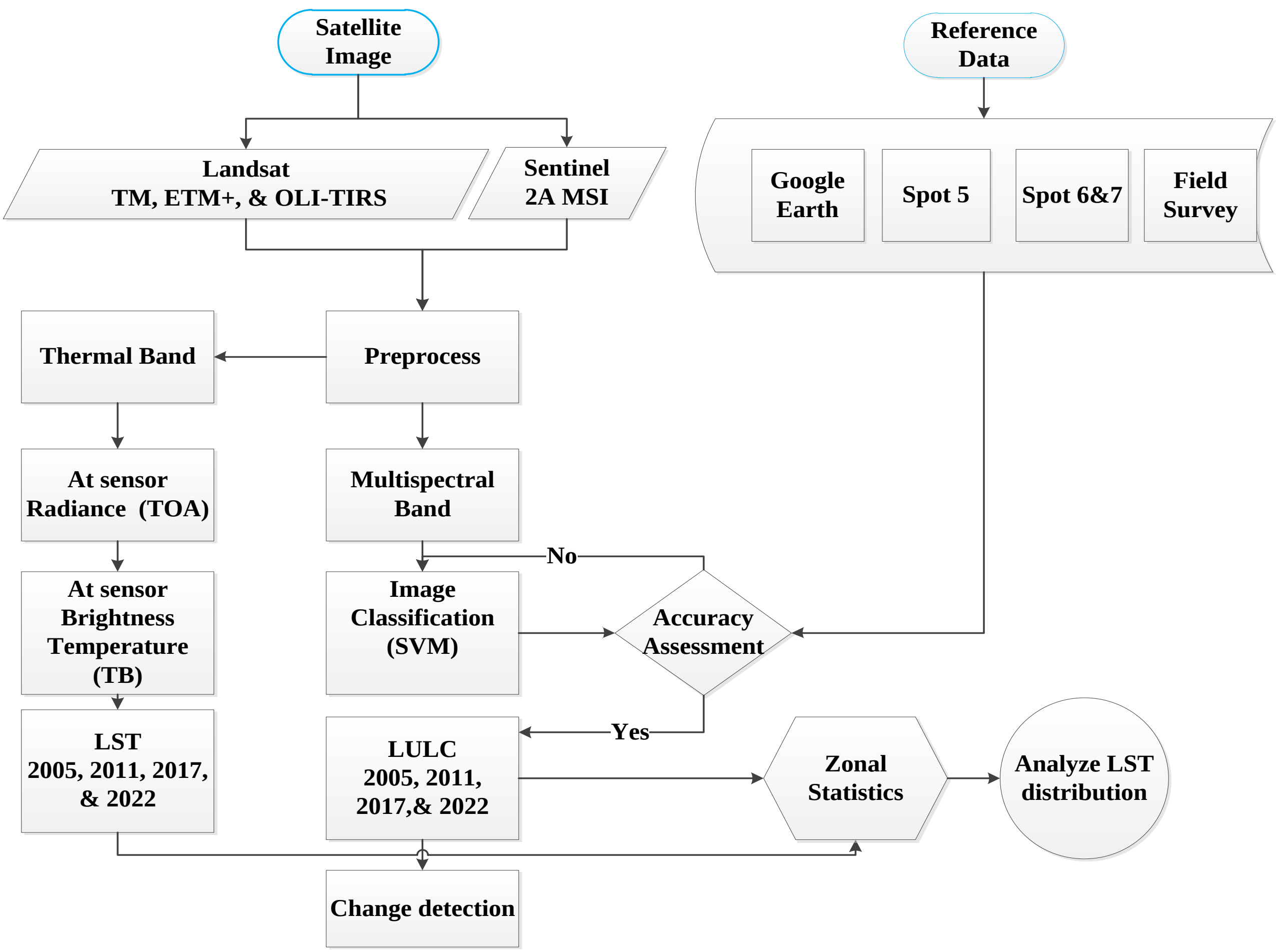


**Figure 2.** Methodology Flowchart.

## 3. Result and Discussion

3.1. LULC Changes (2005 – 2022)

From (Figure 3), we can observe that the area of Agroforestry increased steadily from 104,071 sq. km in 2005 to 105,591 sq. km in 2022. This indicates that agroforestry practices have successfully maintained and even expanded the forest cover while providing for agricultural needs. This suggests that the region actively engages in agroforestry practices to manage the land and maximize productivity sustainably.

On the other hand, the Bareland area decreased from 6725.7 sq. km in 2005 to 4163.13 sq. km in 2011, but it slightly increased again to 5169.78 sq. km in 2022. This suggests that efforts to reforest and restore degraded lands have been partially successful, but more work needs to be done to prevent further deforestation and land degradation. The built-up area has consistently increased, from 1092.6 sq. km in 2005 to 3693.87 sq. km in 2022. The area of Farmland has been decreasing over the years, from 36,515.7 sq. km in 2005 to 33,950.3 sq. km in 2022. This could be due to urbanization, changing agricultural practices, and land degradation.

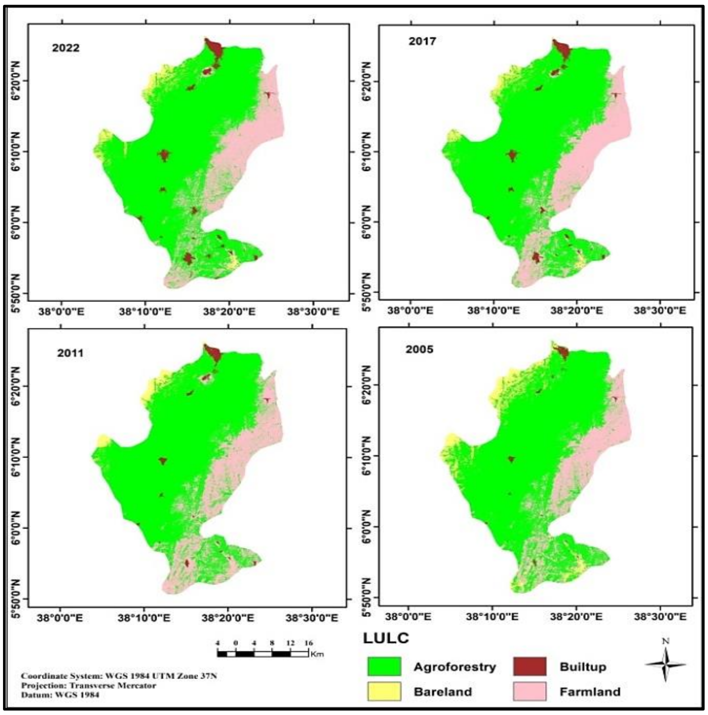


**Figure 3.** Spatial Distribution of LULC

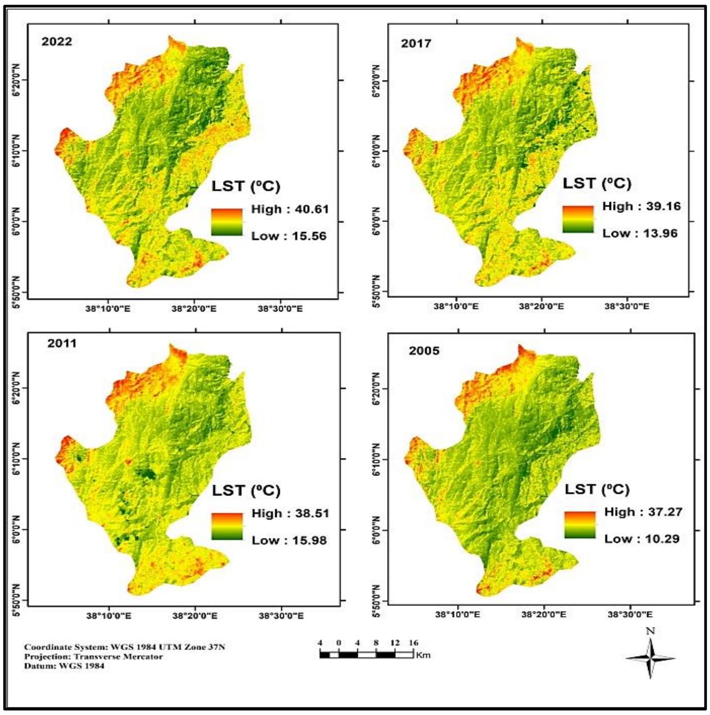


**Figure 4.** Spatial Distribution of LST

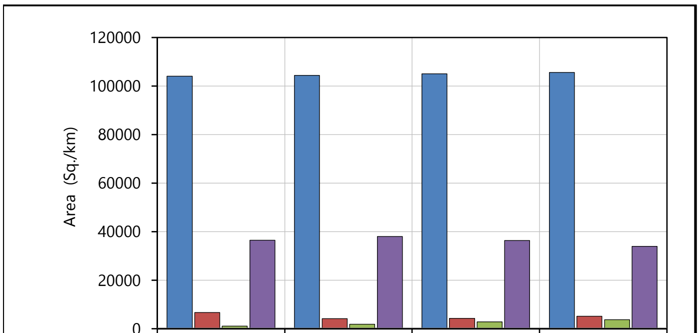


| | 2005 | 2011 | 2017 | 2022 |
|---|---|---|---|---|
| Agroforestry | 104071 | 104347 | 105011 | 105591 |
| Bare Land | 6725.7 | 4163.13 | 4226.94 | 5169.78 |
| Built-up | 1092.6 | 1864.26 | 2801.61 | 3693.87 |
| Farm Land | 36515.7 | 38030.7 | 36364.9 | 33950.3 |

**Figure 5.** Area Coverage of LULC

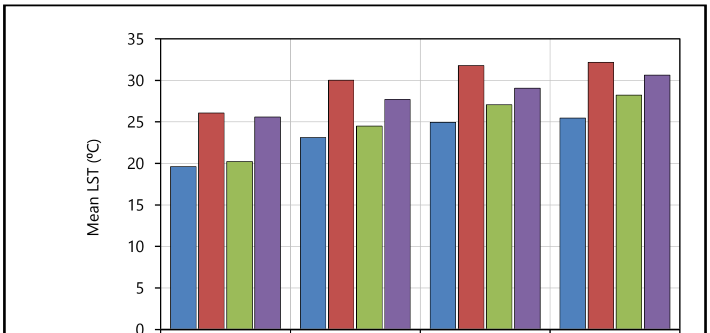


| | 2005 | 2011 | 2017 | 2022 |
|---|---|---|---|---|
| Agroforestry | 19.6 | 23.13 | 24.94 | 25.45 |
| Bare Land | 26.07 | 30.03 | 31.79 | 32.16 |
| Farm Land | 20.23 | 24.5 | 27.05 | 28.23 |
| Built-Up | 25.58 | 27.72 | 29.04 | 30.62 |

**Figure 6.** Mean LST in different LULC

3.2. Spatial Distribution of LST (2005 – 2022)

The average LST in Agroforestry, Bare Land, Farm Land, and Built-up area has progressively increased over the years, from 19.6°C, 26°C, 20.23°C, and 25.58°C in 2005 to 25°C, 32.16°C, 28.23°C and 30.62 in 2022, respectively (Figure 4). The overall result revealed that the average LST in °C has increased from 2005 to 2022.

The maximum change in mean LST was observed between 2005 and 2011. Accordingly, the mean LST increased abruptly by 3.53°C, 3.96°C, 4.27°C, and 2.14°C in Agroforestry, Bare Land, Farm Land, and Built-up respectively, from 2005 to 2011. On the other hand, the minimum mean LST change was detected from 2011 - 2017 and 2017 - 2022. In the last two decades, the mean LST increased even though the coverage area of agroforestry increased; a slight analogous relationship was detected between LST and agroforestry area coverage. Thus, the study results show that LST may not depend only on the local LULC change. Other factors like urbanization and global warming could play a significant role in changing LST locally and globally.

This study's analysis of the LULC dynamics in the Gedeo Zone, dominated by agroforestry, showed a growing demand for land for urban growth. As a result, from 1092.6 sq km in 2005 to 3693.87 sq km in 2022, a larger area was covered by built-up areas. Another Ethiopian study supported this, concentrating on the need for land in Ethiopian cities and towns for urban growth [31].

The coverage of Agroforestry increased steadily from 104,071 sq. km in 2005 to 105,591 sq. km in 2022. This indicates that agroforestry practices have successfully maintained and even expanded the forest cover while providing for agricultural needs [29]. This suggests that the region actively engages in agroforestry practices to manage the land and sustainably maximize productivity [32].

The overall analysis of the LST distribution result revealed that the mean LST in °C has increased from 2005 to 2022. This could be due to urbanization, changing agricultural practices, and land degradation [33], [34]. Even though the area coverage of Agroforestry increased due to the dynamics of other LULC, other factors like global warming could play a vital role in the rise of average LST. Thus, the rise of LST may not depend only on the local LULC change [35], [36]. Other factors like urbanization and global warming could significantly change LST locally and globally [37].

Understanding the impact of LULC on LST is vital for identifying areas where agricultural productivity may be at risk. The Northern areas, including Dilla Town and its surrounding, have experienced significant urbanization, with a maximum recorded mean LST between 2002 and 2022. Understanding the impact of LULC on LST is vital for identifying areas where agricultural productivity may be at risk [38]. The Northwest and Southern parts of the study area, bounded by the West Guji zone, has dominated by Bare Land and negatively influenced agricultural productivity [39]. These areas should be targeted for interventions such as irrigation and shade management. These interventions can help to mitigate the adverse effects of high temperatures on agricultural productivity and ensure sustainable agricultural production in the region.

# 4. Conclusion

The overall dynamics of LULC in the study area indicated a gradual shift towards sustainable practices such as agroforestry, urbanization, and changes in agricultural practices. Policymakers must monitor and manage these changes to ensure sustainable land use and minimize negative environmental and livelihood impacts. From the result of the study, the following conclusions were attained: The area coverage of the built-up area and bare land has increased rapidly while the coverage of agroforestry increased slightly from 2002 to 2022, leading to the rise of LST. The increased area coverage of agroforestry may not guarantee the cooling down of LST; other factors like urbanization and global warming could play a significant role in changing LST locally and globally.

# Acknowledgments

The authors thank the Department of Land Administration and Surveying, College of Agriculture, Dilla University, Ethiopia, for their support during the research. We thank the faculty and staff for providing the resources and facilities for this study. We also thank the data collection surveyors. Their help made this research possible.

# References

[1] G. C. Hulley, D. Ghent, F. M. Göttsche, P. C. Guillevic, D. J. Mildrexler, and C. Coll, “Land Surface Temperature,” in *Taking the Temperature of the Earth*, Elsevier, 2019, pp. 57–127.

[2] G. Hulley and D. Ghent, *Taking the temperature of the earth: steps towards integrated understanding of variability and change*. Elsevier, 2019.

[3] J. Hofierka, M. Gallay, K. Onačillová, and J. Hofierka Jr, “Physically-based land surface temperature modeling in urban areas using a 3-D city model and multispectral satellite data,” *Urban Clim.*, vol. 31, p. 100566, 2020.

[4] J. Tan, D. Yu, Q. Li, X. Tan, and W. Zhou, “Spatial relationship between land-use/land-cover change and land surface temperature in the Dongting Lake area, China,” *Sci. Rep.*, vol. 10, no. 1, pp. 1–9, 2020.

[5] N. R. Govind and H. Ramesh, “The impact of

spatiotemporal patterns of land use land cover and land surface temperature on an urban cool island: a case study of Bengaluru," *Environ. Monit. Assess.*, vol. 191, pp. 1–20, 2019.

[6] R. S. Defries, L. Bounoua, and G. J. Collatz, "Human modification of the landscape and surface climate in the next fifty years," *Glob. Chang. Biol.*, vol. 8, no. 5, pp. 438–458, 2002.

[7] L. Bounoua, R. DeFries, G. J. Collatz, P. Sellers, and H. Khan, "Effects of land cover conversion on surface climate," *Clim. Change*, vol. 52, pp. 29–64, 2002.

[8] E. Pramova, B. Locatelli, H. Djoudi, and O. A. Somorin, "Forests and trees for social adaptation to climate variability and change," *Wiley Interdiscip. Rev. Clim. Chang.*, vol. 3, no. 6, pp. 581–596, 2012.

[9] C. Mbow, P. Smith, D. Skole, L. Duguma, and M. Bustamante, "Achieving mitigation and adaptation to climate change through sustainable agroforestry practices in Africa," *Curr. Opin. Environ. Sustain.*, vol. 6, pp. 8–14, 2014.

[10] S. Sarvade, R. Singh, H. Prasad, and D. Prasad, "Agroforestry practices for improving soil nutrient status," *Pop. Kheti*, vol. 2, no. 1, pp. 60–64, 2014.

[11] N. Sharma, B. Bohra, N. Pragya, R. Ciannella, P. Dobie, and S. Lehmann, "Bioenergy from agroforestry can lead to improved food security, climate change, soil quality, and rural development," *Food Energy Secur.*, vol. 5, no. 3, pp. 165–183, 2016.

[12] T. Thorlakson and H. Neufeldt, "Reducing subsistence farmers' vulnerability to climate change: evaluating the potential contributions of agroforestry in western Kenya," *Agric. Food Secur.*, vol. 1, pp. 1–13, 2012.

[13] K. F. Kalaba, P. Chirwa, S. Syampungani, and C. O. Ajayi, "Contribution of agroforestry to biodiversity and livelihoods improvement in rural communities of Southern African regions," *Trop. rainforests agroforests under Glob. Chang. Ecol. socio-economic valuations*, pp. 461–476, 2010.

[14] A. Raj and S. Chandrawanshi, "Role of agroforestry in poverty alleviation and livelihood support in Chhattisgarh," *South Indian J. Biol. Sci.*, vol. 2, no. 3, pp. 326–330, 2016.

[15] Z. Mekonnen *et al.*, "Traditional knowledge and institutions for sustainable climate change adaptation in Ethiopia," *Curr. Res. Environ. Sustain.*, vol. 3, p. 100080, 2021.

[16] T. K. Kanshie, *Five thousand years of sustainability?: a case study on Gedeo land use (Southern Ethiopia)*. Wageningen University and Research, 2002.

[17] T. Abebe, "Determinants of crop diversity and composition in Enset-coffee agroforestry homegardens of Southern Ethiopia," 2013.

[18] S. Degefa, "Home garden agroforestry practices in the Gedeo zone, Ethiopia: a sustainable land management system for socio-ecological benefits," *Socio-ecological Prod. landscapes seascapes Africa*, p. 28, 2016.

[19] M. Negash, E. Yirdaw, and O. Luukkanen, "Potential of indigenous multistrata agroforests for maintaining native floristic diversity in the south-eastern Rift Valley escarpment, Ethiopia," *Agrofor. Syst.*, vol. 85, pp. 9–28, 2012.

[20] G. M. Foody and A. Mathur, "A relative evaluation of multiclass image classification by support vector machines," *IEEE Trans. Geosci. Remote Sens.*, vol. 42, no. 6, pp. 1335–1343, 2004.

[21] S. S. Keerthi, O. Chapelle, D. DeCoste, K. P. Bennett, and E. Parrado-Hernández, "Building support vector machines with reduced classifier complexity.," *J. Mach. Learn. Res.*, vol. 7, no. 7, 2006.

[22] K. S. Kumar, P. U. Bhaskar, and K. Padmakumari, "Estimation of land surface temperature to study urban heat island effect using LANDSAT ETM+ image," *Int. J. Eng. Sci. Technol.*, vol. 4, no. 2, pp. 771–778, 2012.

[23] J. C. Jiménez-Muñoz, J. A. Sobrino, D. Skoković, C. Mattar, and J. Cristobal, "Land surface temperature retrieval methods from Landsat-8 thermal infrared sensor data," *IEEE Geosci. Remote Sens. Lett.*, vol. 11, no. 10, pp. 1840–1843, 2014.

[24] A. Rajeshwari and N. D. Mani, "Estimation of land surface temperature of Dindigul district using Landsat 8 data," *Int. J. Res. Eng. Technol.*, vol. 3, no. 5, pp. 122–126, 2014.

[25] M. B. Giannini, O. R. Belfiore, C. Parente, and R. Santamaria, "Land Surface Temperature from Landsat 5 TM images: comparison of different methods using airborne thermal data.," *J. Eng. Sci. Technol. Rev.*, vol. 8, no. 3, 2015.

[26] Q. Weng, D. Lu, and J. Schubring, "Estimation of land surface temperature–vegetation abundance relationship for urban heat island studies," *Remote Sens. Environ.*, vol. 89, no. 4, pp. 467–483, 2004.

[27] R. R. Jensen, J. D. Gatrell, D. D. McLean, Q. Weng, and R. C. Larson, "Satellite remote sensing of urban heat islands: current practice and prospects," *Geo-spatial Technol. urban Environ.*, pp. 91–111, 2005.

[28] D. Skoković *et al.*, "Calibration and Validation of land surface temperature for Landsat8-TIRS sensor," *L. Prod. Valid. Evol.*, 2014.

[29] Y. Xiong, S. Huang, F. Chen, H. Ye, C. Wang, and C. Zhu, "The impacts of rapid urbanization on the thermal environment: A remote sensing study of Guangzhou, South China," *Remote Sens.*, vol. 4, no. 7, pp. 2033–2056, 2012.

[30] J. C. Jiménez-Muñoz, J. A. Sobrino, A. Plaza, L. Guanter, J. Moreno, and P. Martínez, "Comparison between fractional vegetation cover retrievals from vegetation indices and spectral mixture analysis: Case study of PROBA/CHRIS data over an agricultural area," *Sensors*, vol. 9, no. 02, pp. 768–793, 2009.

[31] B. K. Terfa, N. Chen, D. Liu, X. Zhang, and D. Niyogi, "Urban expansion in Ethiopia from 1987 to 2017: Characteristics, spatial patterns, and driving forces," *Sustainability*, vol. 11, no. 10, p. 2973, 2019.

[32] T. S. Shanka, "Characterizing to sustain the agrobiodiversity in the Gedeo Zone, Southern Ethiopia," in *Natural Resources Conservation and Advances for Sustainability*, Elsevier, 2022, pp. 581–612.

[33] B. Tsegaye, "Effect of land use and land cover changes on soil erosion in Ethiopia," *Int. J. Agric. Sci. Food Technol.*, vol. 5, no. 1, pp. 26–34, 2019.

[34] S. B. Wassie, "Natural resource degradation tendencies in

Ethiopia: a review," *Environ. Syst. Res.*, vol. 9, pp. 1–29, 2020.
[35] R. Alkama and A. Cescatti, "Biophysical climate impacts of recent changes in global forest cover," *Science (80-. ).*, vol. 351, no. 6273, pp. 600–604, 2016.
[36] S. Yin, W. Wu, X. Zhao, C. Gong, X. Li, and L. Zhang, "Understanding spatiotemporal patterns of global forest NPP using a data-driven method based on GEE," *PLoS One*, vol. 15, no. 3, p. e0230098, 2020.
[37] N. E. A. Murray, M. B. Quam, and A. Wilder-Smith, "Epidemiology of dengue: past, present and future prospects," *Clin. Epidemiol.*, pp. 299–309, 2013.
[38] A. Parven *et al.*, "Impacts of disaster and land-use change on food security and adaptation: Evidence from the delta community in Bangladesh," *Int. J. Disaster Risk Reduct.*, vol. 78, p. 103119, 2022.
[39] A.-A. Kafy *et al.*, "Assessment and prediction of seasonal land surface temperature change using multi-temporal Landsat images and their impacts on agricultural yields in Rajshahi, Bangladesh," *Environ. Challenges*, vol. 4, p. 100147, 2021.

## Abbreviations/Acronyms

| | | |
|---|---|---|
| DN | : | Digital Number |
| DOS | : | Dark Object Subtraction |
| ESA | : | European Space Agency |
| EROS | : | Earth Resources Observation System |
| ETM | : | Enhanced Thematic Mapper |
| GIS | : | Geographic Information Science |
| GII | : | Geospatial Information Institute |
| GPS | : | Global Positioning System |
| LST | : | Land Surface Temperature |
| LULC | : | Land Use Land Cover |
| MSI | : | Multi-Spectral Instrument |
| OLI | : | Operational Land Imager |
| SNNP | : | Southern Nations Nationalities and Peoples |
| SVM | : | Support Vector Machine |
| TIRS | : | Thermal Infrared Sensor |
| TM | : | Thematic Mapper |